Indian Journal of Heterocyclic Chemistry
Vol. 30 - Number 04 (Oct-Dec 2020) 489-502
DocID: https://connectjournals.com/01951.2020.30.489

ISSN (Print) : 0971-1627
ISSN (Online) : 2456-4311

In silico Investigation of Therapeutic Potentials of Coumarin-Quinoxaline Hybrids against Breast Cancer, Synthesis and *In vitro* Activity

Rohit Bhatia[1,2], Raj K. Narang[2], Ravindra K. Rawal[3]*

[1]Department of Pharmaceutical Sciences and Technology, MRSPTU, Bathinda, Punjab, India
[2]Department of Pharmaceutical Chemistry, ISF College of Pharmacy, Ferozepur G.T. Road, Moga, Punjab, India
[3]Department of Chemistry, Maharishi Markandeshwar (Deemed to be University), Mullana, Haryana, India

ABSTRACT To explore the aromatase and HER2 inhibitory activity and to develop newer drug candidates, we have designed a library of ninety compounds by hybridization of two heterocyclic scaffolds; coumarin and quinoxaline. The different derivatives were designed by making substitutions on both the moieties. The designed compounds were further subjected to molecular docking studies against aromatase (PDB Id: 3S7S) and HER2 (PDB Id: 3WSQ) using molecular operating environment 2019.0102 software. Seven compounds revealed best docking scores and their binding patterns in the pocket of aromatase were determined and compared with the standard drugs. Further, *in silico* drug likeliness properties and toxicity profile of best compounds were established using preADME, swissADME, and Protox softwares. The docking protocol was validated and the RMSD value was found to be 1.34. The best four compounds were further synthesized and evaluated for *in vitro* activity against breast cancer utilizing MCF7 and T47D cell lines. The compounds revealed moderate to good activity. The best four compounds were synthesized in the laboratory.

KEYWORDS Aromatase, Coumarin, Drug likeliness, Molecular operating environment, Quinoxaline.

How to cite this article: Bhatia, R., Narang, R.K., Rawal, R.K. *In silico* Investigation of Therapeutic Potentials of Coumarin-quinoxaline Hybrids against Breast Cancer, Synthesis and *In vitro* Activity, *Indian J. Heterocycl. Chem.*, **2020**, *30*, 489–502. *(DocID: https://connectjournals.com/01951.2020.30.489)*

INTRODUCTION

Breast cancer is one of the most frequent and insidious cancer in women.[1] It impacts about 2.1 million women per year and is one of the most lethal ailments in women. According to the WHO, about 627,000 women died globally in 2018 due to breast cancer which constituted 15% of all deaths due to cancer among women.[2] It has been estimated that about 66% postmenopausal women suffering from breast cancer are associated with estrogen dependent breast cancer. Estrogen binds to the estrogen receptors (present in mammary glands) and promotes the tumor growth in female breasts.[3] Estrogens cause enhancement of proliferation of breast epithelial cells and estrogen dependent mammary carcinoma cells and secrete various growth factors.[4] Aromatase is a cytochrome P450 enzyme complex which is present in large concentrations in ovaries of premenopausal women, in peripheral adipose tissues of postmenopausal women and in the placenta of pregnant women.[5] It has been also reported that aromatase activity is maximum in or near the tumor sites in breasts.[6,7] Aromatase enzyme acts on the androgens and produces the most potent endogenous estrogen estradiol.[8] A continuous research is in progress to develop newer drug candidates with promising activity against breast cancer. Many research groups have focused on inhibition of aromatase for drug design and development. A few aromatase inhibitors have been already available in market such as anastrozole, letrozole, exemestane, and testolactone.[9] Another enzyme

*Corresponding author: E-mail: rawal.ravindra@gmail.com

Published & Hosted by :
Journal Homepage :
www.connectjournals.com/ijhc
www.connectjournals.com

which is associated with the development of tumors in breast cells is human protein kinase. Various forms of this kinase such as vascular endothelial growth factor receptor (VEGFR), c-Met, platelet-derived growth factor receptor (PDGFR), and human epidermal growth factor receptor (EGFR/HER-2) are associated with breast cancers. HER2 is a type of protein kinase which promotes proliferation and survival of tumor and lesions which ultimately lead to metastases.[10,11] Although there is tremendous advancements that have been achieved by developing various cytotoxic agents, chemotherapeutic agents, endocrine therapies, and molecular inhibitors, still the metastatic breast cancer is the major lethal ailment in postmenopausal women.[12-15] Beyond this, specificity and toxicity issues are also there with the existing drugs. Therefore, to develop target specific therapeutic candidates with least toxicity is the requirement of the hour to cure this disease. Many researchers have explored various heterocyclic compounds to get maximum therapeutic efficacy from them. With a vision of novel drug design, the concept of molecular hybridization is a significant approach which involves combination of two structurally diverse motifs in a single molecule with excellent therapeutic potential.[16] It is well evident from the literature that coumarin scaffold possesses significant anticancer activity and also has aromatase inhibition potential.[17-20]

Coumarin is a versatile heterocycle and possesses many sites which enable it to combine with other potent moieties to construct a hybrid molecule. The moieties in a hybrid may have different mode of actions or may bind to different targets to get desired biological activity. Many coumarin hybrids with different moieties have been reported with promising activity against breast cancer. A few reported coumarin hybrids against breast cancer are depicted in **Figure 1**.[1] Quinoxaline is another potent scaffold which has been explored by several research groups for its anti-cancer potentials. Many reports are available in the literature revealing its promising activity against breast cancer.[21,22] Quinoxaline exhibits its anti-cancer potentials by inhibiting human protein kinases which are responsible for cell proliferation, migration, and differentiation.[10,11,23-26] Quinoxaline derivatives also stimulate production of reactive oxygen species (ROS) resulting into cell apoptosis and cytotoxicity.[27]

In the present work, with a view point of new drug candidate discovery, we have designed a library of 90 coumarin-quinoxaline hybrids to explore the therapeutic potentials of both the motifs in a single molecule. Molecular docking studies are very much significant to predict the binding patterns of the designed compounds with its target and also to get idea about potency of the compounds. As coumarins have tendency to inhibit aromatase as well as protein kinase and quinoxaline inhibits HER2; the designed compounds were subjected to docking against both of these targets. The rationale behind the design of these hybrids is just to get maximum activity against breast cancer by blocking both of the targets **[Figure 2]**. The compounds

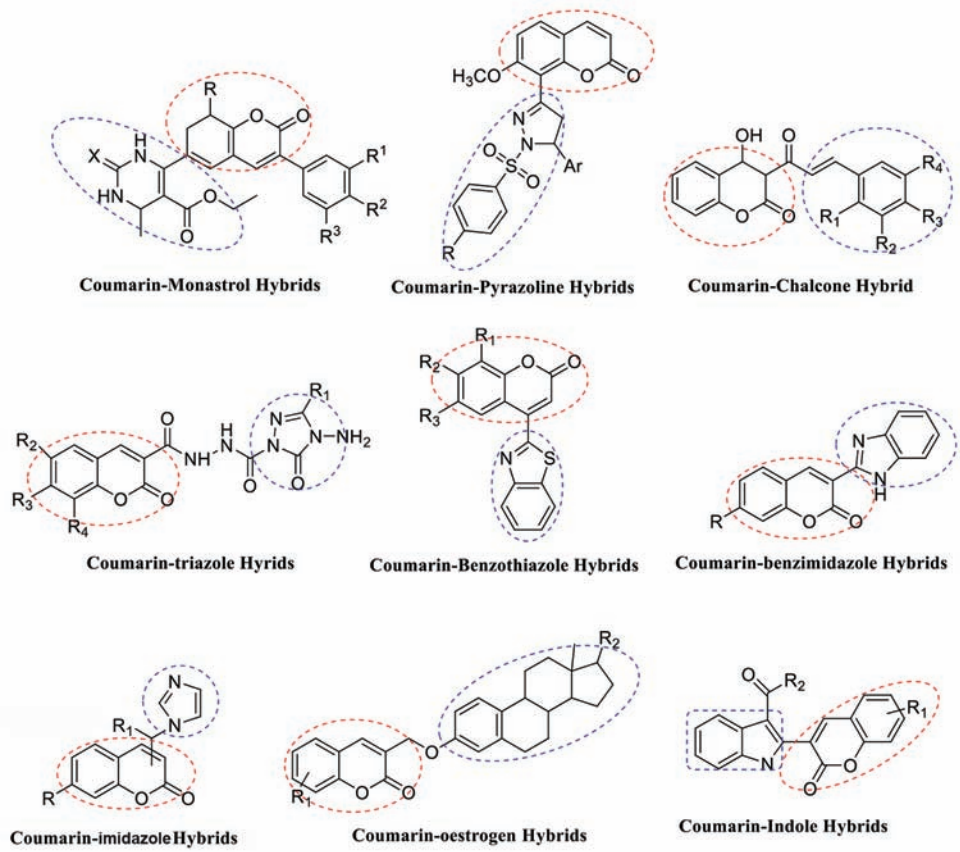

Figure 1: Some coumarin hybrid compounds against breast cancer

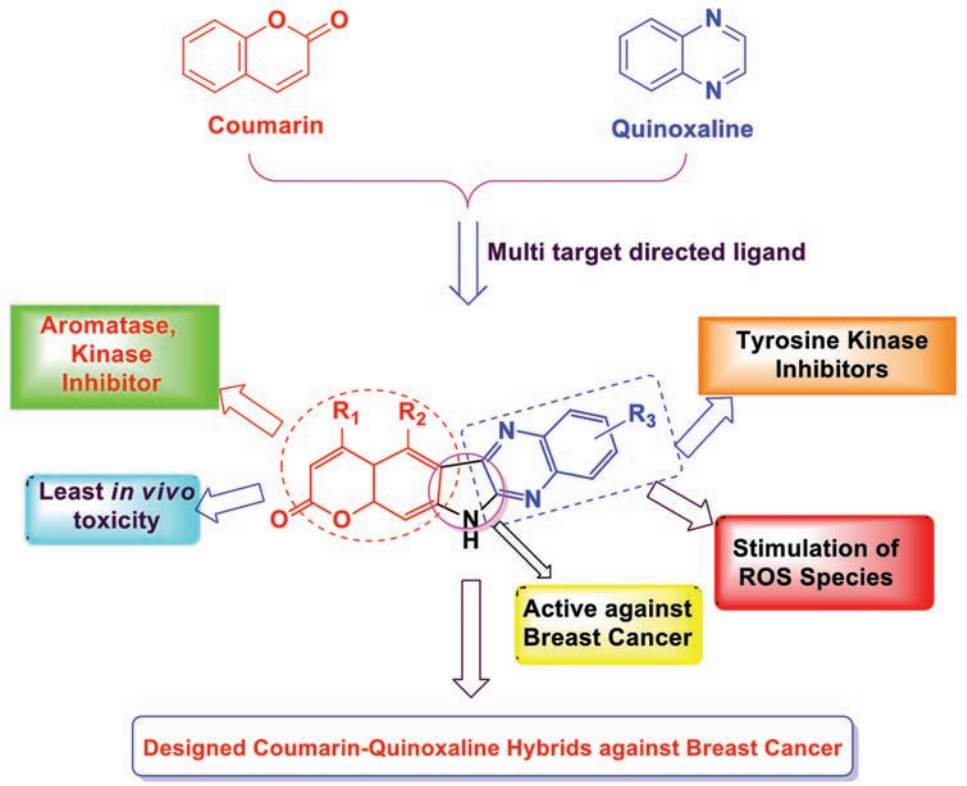

Figure 2: Rationale behind the design of coumarin-quinoxaline hybrids

displaying best docking scores were further studied for 2D and 3D binding patterns, *in silico* drug likeliness, ADME, and toxicity predictions. The best four compounds were further synthesized and evaluated for *in vitro* activity against breast cancer.

RESULTS AND DISCUSSION

Interactions of designed molecules with aromatase and HER2

Molecular docking studies of designed molecules were carried out against human aromatase (PDB Id: 3S7S) and human epidermal growth receptor-2 (PDB Id: 3WSQ) to evaluate the binding patterns of the molecules with the receptor. Various docking scores of designed molecules RB1-RB90 **[Figure 3]** calculated by MOE software against both the protein IDs are displayed in **Table 1**. The docking protocol was validated by re-docking of internal ligand over the cocrystallized ligand and the RMSD value was found to be 1.34. The docking scores of all the designed hybrids were compared to the standard drugs exemestane (aromatase inhibitor) and trastuzumab (HER2 inhibitor).

Among the 90 designed molecules, seven displayed maximum docking scores which were comparable to the standard drugs. These seven were predicted to have maximum inhibitory potentials against both the receptors. The selected seven hybrid molecules were further analyzed for the binding patterns within the cavities of the receptors. Various interactions displayed by the seven best compounds at particular distances, are depicted in **Table 2**. The interaction poses of compounds with maximum docking

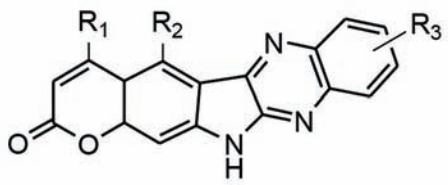

Figure 3: Designed Compounds RB1-RB90

scores **(RB14, RB86)** for PDB Id:3S7S are presented in **Figures 4 and 5** and compounds revealing maximum docking scores **(RB16, RB36)** for PDB Id: 3WSQ, in **Figures 6 and 7**. The main amino residues involved in bonding in the pocket of aromatase were Val370, Met311, Gly439, Met303, Ala307, and Ser314 whereas in the pocket of HER2 Val164, Arg143, Pro41, Pro172, Ala173, Gly42, Ala85, Glu162, and Tyr181. The major interactions types were hydrogen bonding, arene-cation, and arene-H interactions. It is evident that the pattern of binding in case of standard drug exemestane involved similar amino acid residues and functional groups as in case of best compounds against aromatase **[Figure 8]**. The same trend was observed in case of HER2 receptor where the standard drug trastizumab was used **[Figure 9]**. The overlay pose of internal ligand of aromatase and re-docked ligand is depicted in **Figure 10**. Compound RB86 revealed the best docking score against both the receptor.

On the basis of predicted docking scores and binding patterns of the designed compounds with the receptors the structural activity relationship were explained as: Incorporation of methoxy (-OCH_3), hydroxyl (-OH),

Table 1: Docking scores of designed library of compounds

Compound No.	R_1	R_2	R_3	Docking Score (PDB Id: 3S7S)	Docking Score (PDB Id: 3WSQ)
RB1	H	H	H	−7.63	-6.99
RB2	H	H	4-CH_3	−7.12	-6.82
RB3	H	H	4-F	−7.28	−6.72
RB4	H	H	4-CF_3	−7.04	−6.98
RB5	H	H	4,5-$(CH_3)_2$	−6.99	−6.63
RB6	H	H	3-OCH_3	−6.82	−6.12
RB7	H	H	3,4-$(OCH_3)_2$	−7.18	−6.28
RB8	H	H	4-Cl	−6.72	−6.04
RB9	H	H	4-Br	−6.98	−5.98
RB10	H	H	4-NO_2	−7.14	−5.76
RB11	OCH_3	H	H	−7.22	−5.78
RB12	OCH_3	H	3-CH_3	−7.28	−5.92
RB13	**OCH_3**	**H**	**4-F**	**−8.72**	**−7.48**
RB14	**OCH_3**	**H**	**4-CF_3**	**−8.92**	**−7.58**
RB15	OCH_3	H	2,3-$(CH_3)_2$	−7.69	−7.26
RB16	**OCH_3**	**H**	**3-OCH_3**	**−8.68**	**−7.76**
RB17	**OCH_3**	**H**	**3,4-$(OCH_3)_2$**	**−8.82**	**−7.68**
RB18	OCH_3	H	4-Cl	−8.42	−7.44
RB19	**OCH_3**	**H**	**4-Br**	**−8.66**	**−7.52**
RB20	OCH_3	H	4-NO_2	−8.12	−7.13
RB21	OH	H	H	−7.96	−6.88
RB22	OH	H	4-CH_3	−7.88	−6.08
RB23	OH	H	4-F	−7.62	−6.38
RB24	OH	H	4-CF_3	−7.74	−6.22
RB25	OH	H	4,5-$(CH_3)_2$	−7.19	−5.76
RB26	OH	H	3-OCH_3	−7.32	−5.89
RB27	OH	H	3,4-$(OCH_3)_2$	−8.02	−5.98
RB28	OH	H	4-Cl	−7.84	−6.48
RB29	OH	H	4-Br	−7.86	−6.56
RB30	OH	H	4-NO_2	−7.12	−5.42
RB31	C_6H_5	H	H	−6.78	−5.12
RB32	C_6H_5	H	4-CH_3	−6.98	−5.08
RB33	C_6H_5	H	4-F	−7.42	−6.14
RB34	C_6H_5	H	4-CF_3	−7.56	−6.66
RB35	C_6H_5	H	4,5-$(CH_3)_2$	−7.96	−6.92
RB36	**C_6H_5**	**H**	**3-OCH_3**	**−8.76**	**−7.98**
RB37	C_6H_5	H	3,4-$(OCH_3)_2$	−7.98	−6.88
RB38	C_6H_5	H	4-Cl	−6.72	−5.62
RB39	C_6H_5	H	4-Br	−6.88	−5.87
RB40	C_6H_5	H	4-NO_2	−6.78	−5.73
RB41	H	CH_3	H	−7.22	−6.42
RB42	H	CH_3	4-CH_3	−7.16	−6.26
RB43	H	CH_3	4-F	−7.62	−6.60
RB44	H	CH_3	4-CF_3	−7.76	−6.86
RB45	H	CH_3	4,5-$(CH_3)_2$	−7.82	−7.82
RB46	H	CH_3	3-OCH_3	−7.89	−7.89
RB47	H	CH_3	3,4-$(OCH_3)_2$	−7.66	−7.66
RB48	H	CH_3	4-Cl	−6.18	−6.18

(*Contd...*)

Table 1: (*Continued*)

Compound No.	R_1	R_2	R_3	Docking Score (PDB Id: 3S7S)	Docking Score (PDB Id: 3WSQ)
RB49	H	CH_3	4-Br	−6.99	−6.99
RB50	H	CH_3	4-NO_2	−6.76	−6.76
RB51	CH_3	CH_3	H	−6.56	−6.56
RB52	CH_3	CH_3	4-CH_3	−6.65	−6.65
RB53	CH_3	CH_3	4-F	−6.79	−6.79
RB54	CH_3	CH_3	4-CF_3	−7.13	−6.52
RB55	CH_3	CH_3	4,5-$(CH_3)_2$	−7.14	−5.74
RB56	CH_3	CH_3	3-OCH_3	−7.78	−6.67
RB57	CH_3	CH_3	3,4-$(OCH_3)_2$	−7.84	−6.72
RB58	CH_3	CH_3	4-Cl	−7.04	−5.18
RB59	CH_3	CH_3	4-Br	−7.08	−5.62
RB60	CH_3	CH_3	4-NO_2	−7.16	−5.98
RB61	OH	CH_3	H	−5.99	−5.12
RB62	OH	CH_3	4-CH_3	−6.14	−5.13
RB63	OH	CH_3	4-F	−6.13	−5.02
RB64	OH	CH_3	4-CF_3	−6.34	−5.16
RB65	OH	CH_3	4,5-$(CH_3)_2$	−6.42	−5.34
RB66	OH	CH_3	3-OCH_3	−6.98	−5.72
RB67	OH	CH_3	3,4-$(OCH_3)_2$	−7.02	−6.14
RB68	OH	CH_3	4-Cl	−6.86	−5.78
RB69	OH	CH_3	4-Br	−6.82	−5.72
RB70	OH	CH_3	4-NO_2	−6.92	−5.88
RB71	H	OCH_3	H	−6.73	−5.64
RB72	H	OCH_3	4-CH_3	−6.98	−5.34
RB73	H	OCH_3	4-F	−8.02	−6.78
RB74	H	OCH_3	4-CF_3	−7.88	−6.62
RB75	H	OCH_3	4,5-$(CH_3)_2$	−7.14	−5.67
RB76	H	OCH_3	3-OCH_3	−7.26	−5.99
RB77	H	OCH_3	3,4-$(OCH_3)_2$	−7.98	−6.12
RB78	H	OCH_3	4-Cl	−7.24	−5.78
RB79	H	OCH_3	4-Br	−7.12	−5.42
RB80	H	OCH_3	4-NO_2	−7.24	−5.48
RB81	OH	OCH_3	H	−7.98	−5.93
RB82	OH	OCH_3	4-CH_3	−7.73	−5.78
RB83	OH	OCH_3	4-F	−7.76	−5.52
RB84	OH	OCH_3	4-CF_3	−7.89	−5.79
RB85	OH	OCH_3	4,5-$(CH_3)_2$	−7.56	−5.86
RB86	**OH**	**OCH_3**	**3-OCH_3**	**−9.21**	**−7.31**
RB87	OH	OCH_3	3,4-$(OCH_3)_2$	−8.14	−6.99
RB88	OH	OCH_3	4-Cl	−8.12	−6.88
RB89	OH	OCH_3	4-Br	−8.06	−6.76
RB90	OH	OCH_3	4-NO_2	−8.16	−6.18
Exemestane				**−9.18**	
Trastuzumab					**−7.38**

and phenyl groups on 4th position of coumarin scaffold revealed maximum docking scores and orientations against aromatase as well as HER2 receptors. Substitution on 5th position of coumarin scaffold generally does not have any significant effect on binding affinity but when it is substituted with methoxy (-OCH_3), maximum docking score comparable to exemestane was obtained. Substitution of phenyl ring of quinoxaline with fluoro, bromo, trifluoro

Table 2: Various interactions revealed by best seven designed hybrids

Compound	Docking scores		Type of interactions and distances	
	3S7S	3WSQ	3S7S	3WSQ
RB13	−8.72	−7.48	Val370 (H-bond with =O; 2.41Å), Ser314(H-bond with =O; 3.96Å), Met311(H-bond with –NH; 2.19Å), Gly439(H-bond with N; 3.79Å), Met303 (Bond between S and H; 3.80Å), Gly439 (Two Arene-H interactions)	Val164 (Arene-H interaction), Pro41 (Two arene-cation interactions), Val164 (H-bond with NH; 2.83Å), Val164 (H-bond with N; 3.03Å), Arg143 (H-bond with NH; 3.40Å), Arg143 (H-bond with NH; 3.62Å), Arg143 (H-bond with N; 4.22Å)
RB14	−8.92	−7.58	Met311 (H-bond with –NH; 2.64Å), Gly439 (Two Arene-H interactions), Met303(Bond between S and H; 3.95Å), Gly439 (H bond with N; 3.65Å), Met364 (H bond with =O; 2.93Å), Val370 (H-bond with O; 4.40Å), Ala307 (H-bond with N; 4.64Å)	Valine174 (Two Arene-H interactions), Leu175(H bond with N; 3.67Å), Ala173(H bond with NH; 3.88Å), Pro172 (H bond with NH; 4.76Å)
RB16	−8.68	−7.76	Val370 (H-bond with =O; 2.17Å), Val370 (H-bond with =O; 2.54Å), Met311 (H-bond with –NH; 2.05Å), Gly439 (Arene-H interaction), Gly439 (H bond with N; 3.92Å), THR310 (H-bond with –NH; 4.10Å), Ser314 (H-bond with O; 3.86Å)	Arg143 (Two arene-cation interactions), Thr165 (H-bond with –NH; 3.67Å), Val164 (H bond with N; 3.33Å), Gly42 (H bond with N; 3.99Å), Ala85 (H bond with =O; 3.59Å), Arg143 (H-bond with –NH; 2.86Å)
RB17	−8.82	−7.68	Met311 (H-bond with –NH; 2.24Å), Ala307 (H-bond with =O; 3.24Å), Gly439 (H bond with O; 3.81Å), Val370 (H bond with O; 4.62Å)	Valine174 (Two Arene-H interactions), Ala173 (H-bond with –NH; 3.47Å), Val164 (H-bond with O; 2.47Å), Glu162 (H-bond with O; 4.46Å), Tyr181 (H-bond with O; 3.68Å)
RB19	−8.66	−7.52	Gly439 (Two Arene-H interactions), Met311 (H-bond with –NH; 2.37Å), Met303 (Bond between S and H; 3.86Å), Gly439 (H bond with N; 3.72Å), Val370 (H bond with =O; 2.73Å)	Valine174 (Two Arene-H interactions), Val164 (H-bond with Br; 2.48Å), Ala173 (H-bond with –NH; 3.972Å), Leu175 (H-bond with N; 3.79Å), Tyr181 (H-bond with =O; 3.60Å),
RB36	−8.76	−7.98	Met311 (H-bond with –NH; 2.26Å), Met303 (Bond between S and H; 4.05Å), Thr310 (Arene-H interaction), Ala307 (H bond with =O; 4.45Å)	Pro8 (Arene-H interaction), Gly44 (H bond with =O; 4.19Å), Arg143(H bond with N; 2.96Å), Gln167 (H bond with O; 3.15Å)
RB86	−9.21	−7.31	Met311 (H-bond with NH; 2.19Å), Met303(Bond between S and H; 3.75Å), Ser199 (H bond with = O; 3.1Å), Ala307 (H bond with O; 3.46Å), Ser314 (H bond with O; 2.66Å), Ala438 (H bond with O; 3.66Å)	Thr43 (H bond with NH; 2.42Å), Ala4 (H bond with OH; 1.79Å), Tyr95 (H bond with N; 2.98Å), Gly42 (H bond with O; 3.81Å), Gln43 (H bond with =O; 3.92Å)
Exemestane	−9.18		Met374 (H bond with =O; 1.97Å), Arg115 (H bond with =O; 2.63Å), Ala306 (H bond with =O; 4.40Å)	
Trastuzumab		−7.38		Val164 (Arene-H interaction), Val164 (H-bond with NH; 2.02Å), Arg143 (Arene-cation interaction), Arg143 (H-bond with O; 2.33Å), Glu166(H bond with OH; 1.88Å), Ser163 (H bond with NH; 2.30Å)

methyl, methoxy, and di-methoxy groups produced compounds with maximum affinity. It is also evident that fused pyrrolidine ring displayed excellent interactions with both of the receptors. Compound RB86 revealed maximum affinity to both of the receptors equivalent to exemestane and trastuzumab. The predicted SAR of designed molecules is outlined in **Figure 11.**

Drug likeliness prediction

Drug likeliness prediction is a significant qualitative approach in drug design to predict that how "drug like" a compound is. These properties can be controlled by medicinal chemists during drug design and are directly related to characteristics of the drug like bioavailability. *In silico* drug likeliness prediction of best seven designed molecules was carried out using Swiss ADME predictor, as depicted in **Table 3**. Percentage absorption (% ABS) was calculated using formula %ABS = 109- (0.345×TPSA). The designed potent analogues displayed good absorption in the range of 76.5–82.77%. The results revealed that designed potent analogs showed no violation of Lipinski's Rule of Five. These predictions suggested that designed analogues can be utilized to develop drug like candidates.

ADME prediction studies

Pharmacokinetic profile of a drug is of utmost significance to approve it as a suitable therapeutic candidate. Many drugs cannot fulfill the favorable pharmacokinetics and get failed in clinical trials. The preliminary screening of ADME properties of designed drugs is a useful approach to save time, cost as well as the risk of failure. *In silico* ADME properties of best seven compounds were predict using preADMET tool version 2.0 software (preadmet.bmdrc.kr). The calculated values of absorption through various barriers were found within the standard limits for all the seven compounds. Human intestinal absorption value greater than 80% suggests that the compound is well absorbed through intestine. Lower value of blood–brain barrier (BBB) from 0.14–0.90 reveals that the compound cannot cross the blood brain barrier. Caco-2 value between 4 and 70 represents moderate absorption, greater than 70 suggests maximum absorption. The potent compounds with the lower MDCK

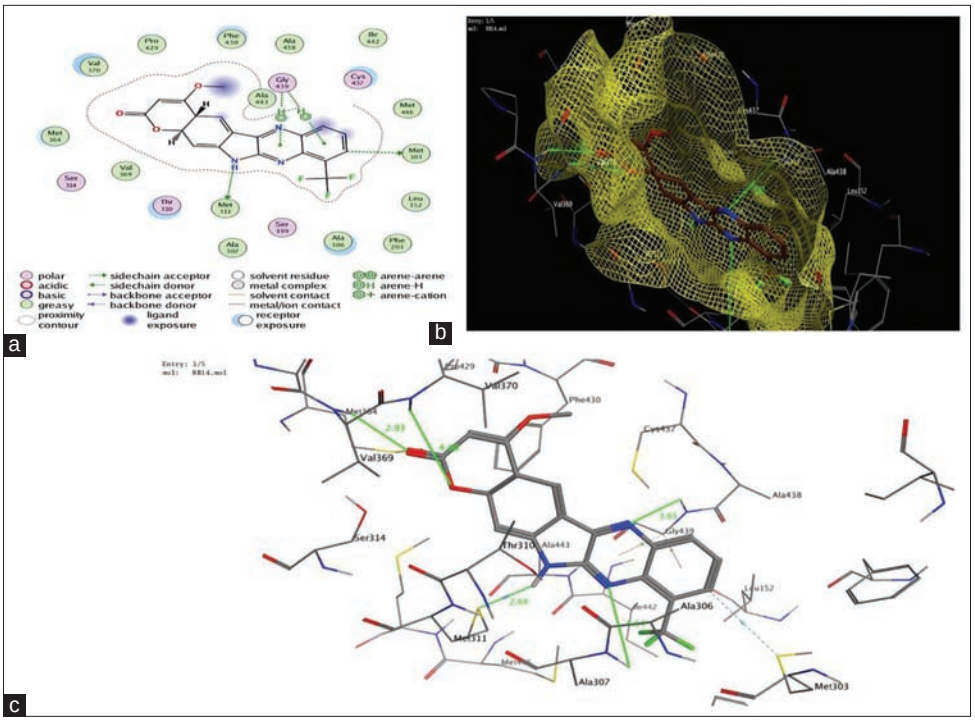

Figure 4: Interaction poses of RB14 with aromatase (a) 2D interactions (b) RB14 embedded in receptor pocket (c) Interactions along with distances

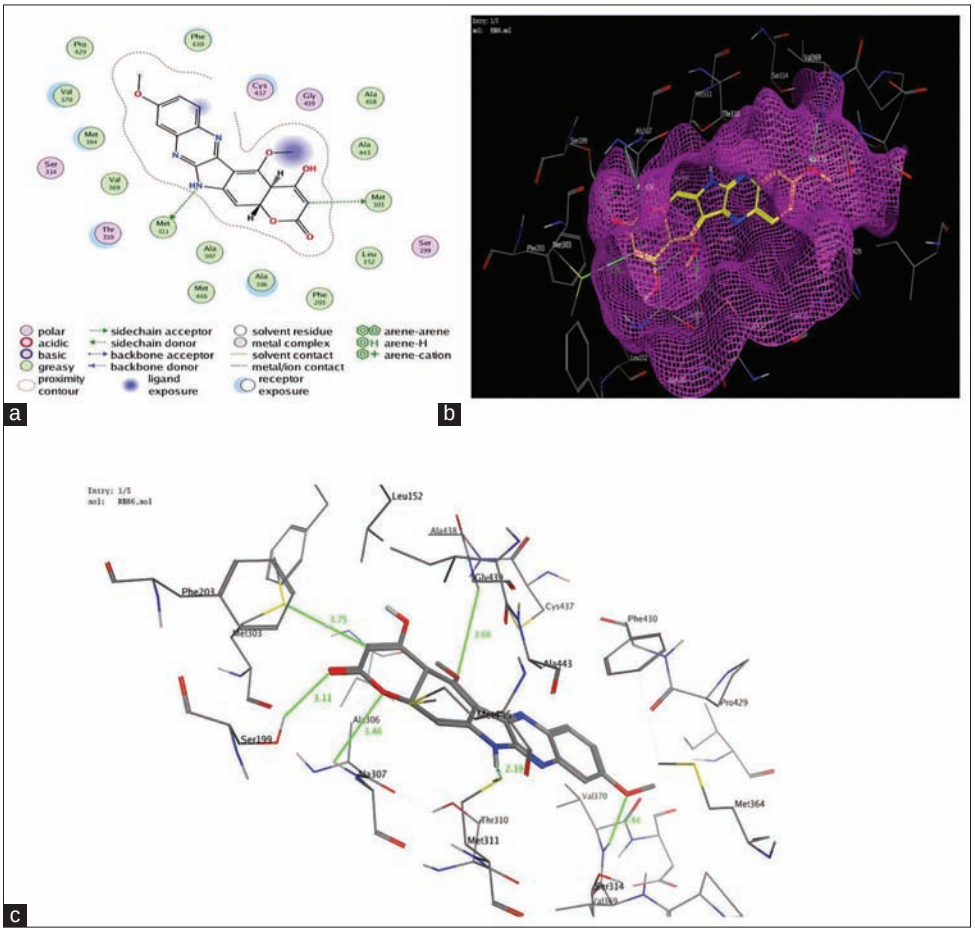

Figure 5: Interaction poses of RB86 with aromatase (a) 2D interactions (b) RB86 embedded in receptor pocket (c) Interactions along with distances

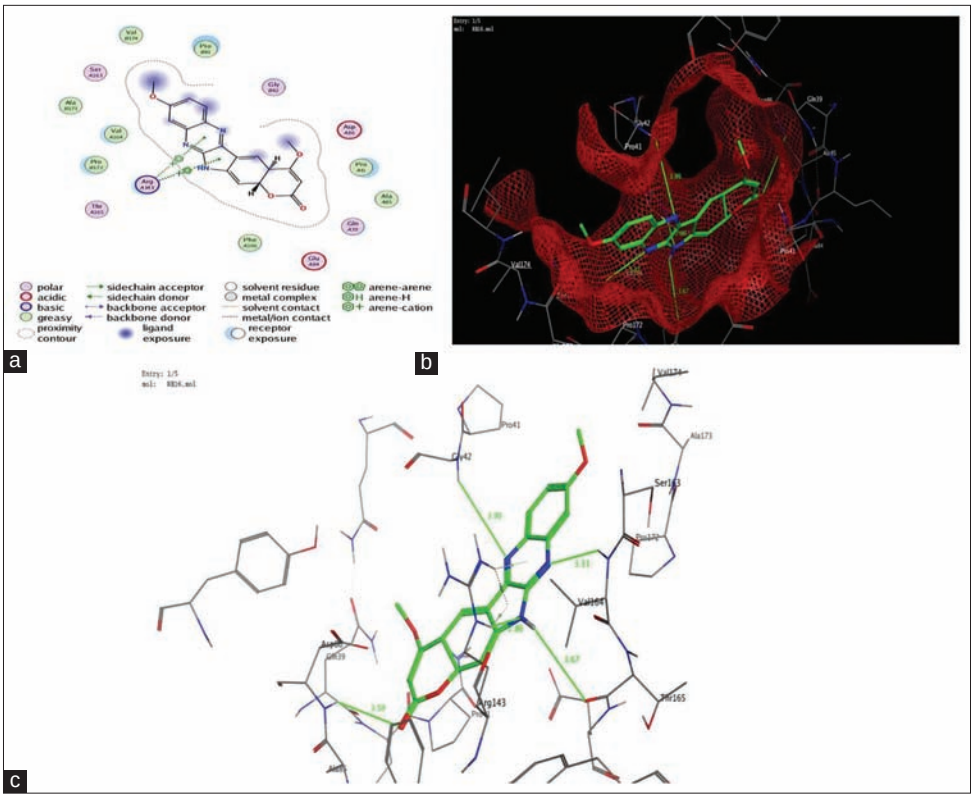

Figure 6: Interaction poses of RB16 with HER2 (a) 2D interactions (b) RB16 embedded in receptor pocket (c) Interactions along with distances

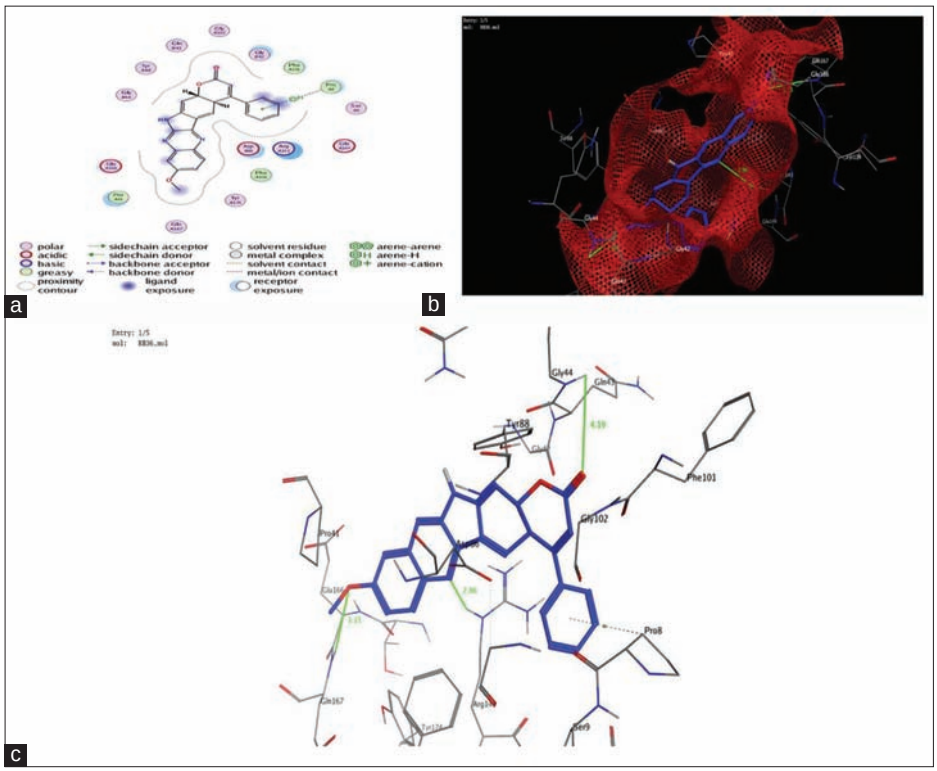

Figure 7: Interaction poses of RB36 with HER2 (a) 2D interactions (b) RB36 embedded in receptor pocket (c) Interactions along with distances

value indicate lower absorption toward kidney cells. Plasma protein binding greater than 85 indicates best distribution properties of potent compounds. The predicted data are compiled in **Table 4.**

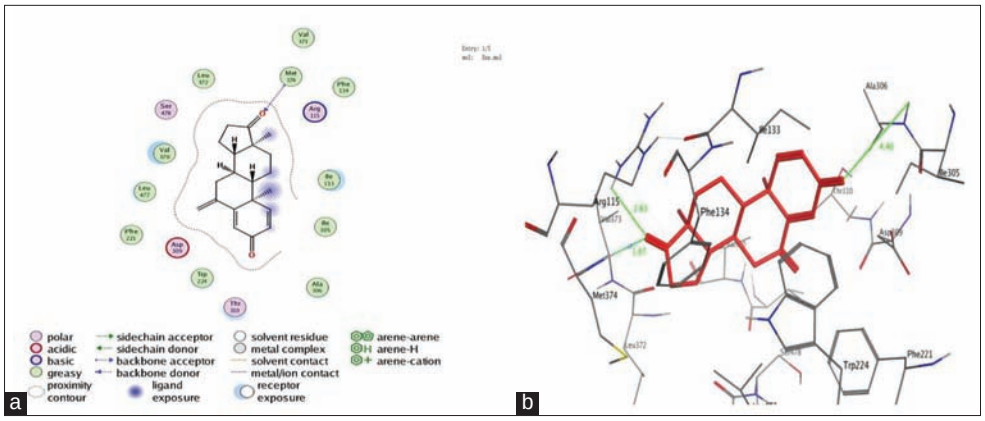

Figure 8: Interaction poses of exemestane with 3S7S (a) 2D interactions (b) Interactions along with distances

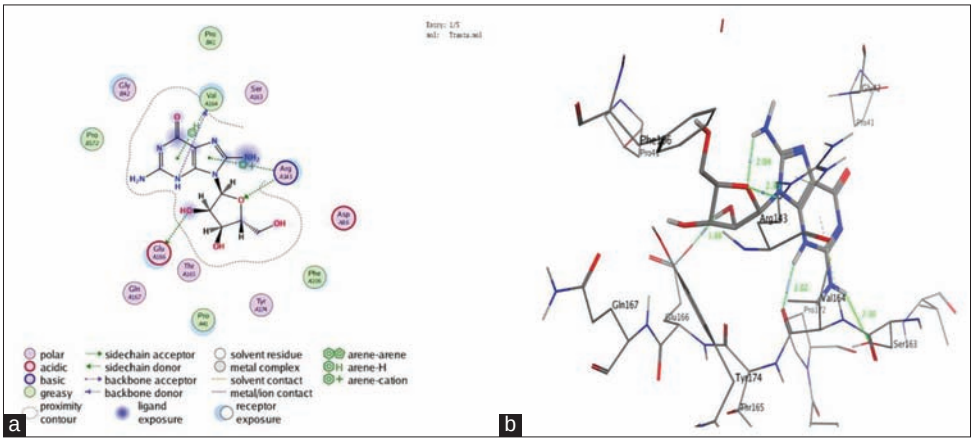

Figure 9: Interaction poses of trastuzumab with 3WSQ (a) 2D interactions (b) Interactions along with distances

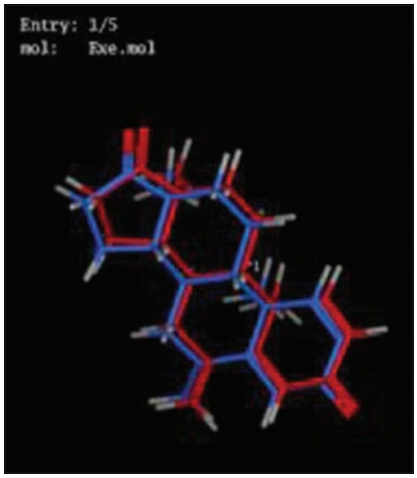

Figure 10: Overlay of internal ligand (red) of aromatase and re-docked ligand (blue)

In silico toxicity prediction

A therapeutic drug is of no use, if it is toxic to other parts of the body although it is effective against particular ailment. Hence, a preliminary idea about the toxicity of a designed molecule is highly useful to avoid failure of it during clinical stages. Toxicity profiling of a drug directly ensures the safety profile of a particular drug. The prediction of toxicity was carried out by PreADME and PROTOX softwares. Protox predictions revealed that the designed compounds lie in Class 4 with LD50 value >900 mg/kg which is much higher dose to be toxic. Rodent toxicity tests for Carcino-Mouse and Carcino-Rat were positive which means there is no evidence of carcinogenic toxicity. Medium risk for hERG inhibition indicates that designed analogues have minimum risk on cardiac action potential. The obtained results from both the sotwares are presented in **Table 5.** From the data, it can be concluded that the designed molecules are safe to be used as a drug.

Synthesis

Compounds **RB14, RB16, RB36,** and **RB86** were synthesized according to the synthetic strategy depicted in **Scheme 1.** The synthesis of intermediate isatin derivatives was carried out according to Sandmeyer's reaction.[28] The physical data (Percentage yield and melting point) of various title compounds are summarized in **Table 6.** Structural characterization of all the title compounds was done using various spectral techniques that including ^{1}H NMR, ^{13}C NMR, and mass spectrometry which fully supported their structural identity.

In vitro anticancer activity

The anti-breast cancer activity of compounds RB14, RB16, RB36, and RB85 was investigated against the human breast cancer cell lines MCF7 and T47D following

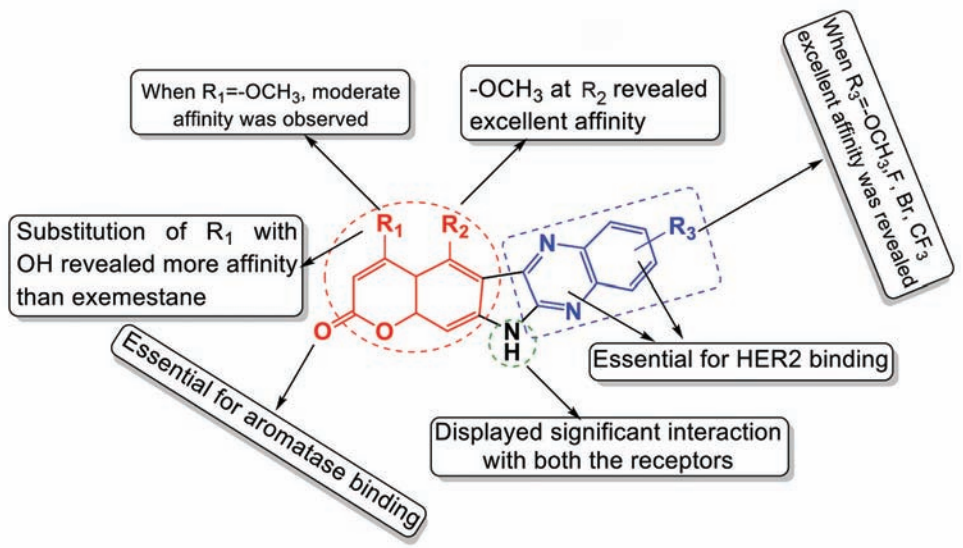

Figure 11: Predicted SAR of designed molecule

Table 3: *In silico* drug like properties of best seven designed molecules

Compound	TPSA[a]	MW[b]	RoB[c]	HBD[d]	HBA[e]	IlogP (MlogP)[f]	logS[g]	% ABS[h]
Rule	≤140	≤500	≤10	≤5	≤10	≤5	>-4	-
RB13	77.10	337.30	1	1	6	2.60	−4.98	82.39
RB14	77.10	387.31	2	1	8	2.82	−5.55	82.39
RB16	86.33	349.34	2	1	6	2.91	−4.81	79.21
RB17	95.56	379.37	3	1	7	3.09	−4.93	76.03
RB19	77.10	398.21	1	1	5	2.86	−5.51	82.39
RB36	77.10	395.41	2	1	5	3.26	−7.17	82.39
RB86	95.56	379.37	3	1	7	2.94	−5.15	76.03

[a]Topological polar surface area; [b]Molecular weight; [c]Number of rotatable bonds; [d]Number of hydrogen bond donors; [e]Number of hydrogen bonds acceptors; [f]Logarithm of compound partition coefficient between n-octanol and water; [g]Logarithm of water solubility; [h]Percentage absorption

Table 4: *In silico* ADME properties of best seven compounds

Compound	HIA%	Caco- 2(nm/sec)	MDCK	BBB (log PS) <0.4	Plasma protein binding (%)
RB13	96.87	23.62	2.32	0.19	90.85
RB14	96.56	21.64	1.68	0.07	93.71
RB16	96.93	28.80	2.78	0.16	70.78
RB17	97.36	30.97	3.92	0.10	58.62
RB19	96.32	22.58	0.3001	0,23	76.19
RB36	96.46	38.18	3.26	0.16	95.12
RB86	93.72	18.12	4.18	0.10	53.25

Table 5: *In silico* toxicity results for best seven compounds

Compound	Carcino-mouse	Carcino-rat	HERG-inhibition	Protox predicted LD50	Protox predicted class
RB13	Positive	Positive	Medium risk	1050 mg/kg	Class 4
RB14	Positive	Positive	Medium risk	920 mg/kg	Class 4
RB16	Positive	Positive	Medium risk	920 mg/kg	Class 4
RB17	Positive	Positive	Medium risk	1000 mg/kg	Class 4
RB19	Positive	Positive	Medium risk	1050 mg/kg	Class 4
RB36	Positive	Positive	Medium risk	1000 mg/kg	Class 4
RB86	Positive	Positive	Medium Risk	1000mg/kg	Class 4

the previously reported colorimetric cytotoxicity assay of Skehan *et al*.[29] The results of cytotoxic activity of the compounds were compared with the standard drugs exemestane and trastuzumab. The IC_{50} values in µg/mL of the compounds and standard drugs are depicted in **Table 7** and **Figure 12a** and **12b**.

Table 6: Physical data of synthesized compounds

Compound	R_1	R_2	R_3	% Yield	Melting point
RB14	OCH_3	H	4-CF_3	66	268–270°C
RB16	OCH_3	H	3-OCH_3	72	298–301°C
RB36	C_6H_5	H	3-OCH_3	56	281–283°C
RB86	OH	OCH_3	3-OCH_3	62	308–310°C

Table 7: Cytotoxic activity of synthesized compounds against breast cancer cell lines

Compound	IC50 (µg/mL)	
	MCF7	T47D
RB14	22.8±2.18	38.82±2.46
RB16	36.8±1.26	29.38±1.02
RB36	12.8±1.12	32.2±1.82
RB86	7.82±0.26	18.6±1.12
Exemestane	2.16±0.32	8.38±0.92
Trastuzumab	9.18±1.02	11.26±1.32

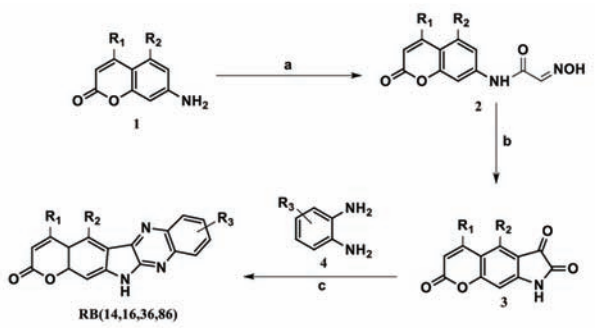

Scheme 1: (a) Chloral hydrate, Na_2SO_4. $HONH_2$.HCl, Reflux 40–45 min (b) H_2SO_4, stirring at 80°C (c) Glacial acetic acid, Reflux 24 h

The results revealed that compounds showed good to moderate cytotoxicity activity against breast cancer cell lines. Compound **RB86** was found most potent among the synthesized compounds against both cell lines. Other compounds showed moderate to weaker activity as compared to standard drugs. Hence, it can be concluded that the presence of electron releasing groups on coumarin as well as quinoxaline moiety has improved impact on cytotoxic activity.

EXPERIMENTAL

Molecular docking

A series of 90 coumarin-quinoxaline hybrid molecules was designed by making different substitutions on different positions. The designed molecules were further subjected to molecular docking against aromatase and HER-2.

Preparation of protein

The 3D crystal structures of aromatase (PDB Id: 3S7S) and HER2 (PDB Id: 3WSQ) were procured from RCSB-PDB (http:/www.rcsb.org/pdb) in pdb format.[30] The protein cavity was prepared using molecular operating environment (MOE) version 2019.0102 by selecting the ligand nearby area up to 10Å. The sequence of steps involved addition of hydrogens, deleting the internal ligands, deletion of waters/cofactors, and isolation of atoms. 3D structures of prepared cavities of both proteins are depicted in **Figure 13.**

Preparation of ligand

The 2D structures of designed compounds were drawn in Chemdraw Professional 15.0 software and were saved as mol files. The 90 ligands were designed and subjected to energy minimization in MOE software by choosing MMFF94x forcefield, Austin model 1 with gradient value of 0.0001 kcal/mol. The energy minimized ligands were saved as tripos mol2 files and converted into mdb.mol files.

Docking of designed ligands and validation

Docking of energy minimized ligands was carried out on aromatase and HER2 using MOE 2019.0102 software. Various sequence of steps involved selection of receptor, selection of site, selection of ligand file, and run. The docking protocol was validated by reproducing the confirmation of internal ligand

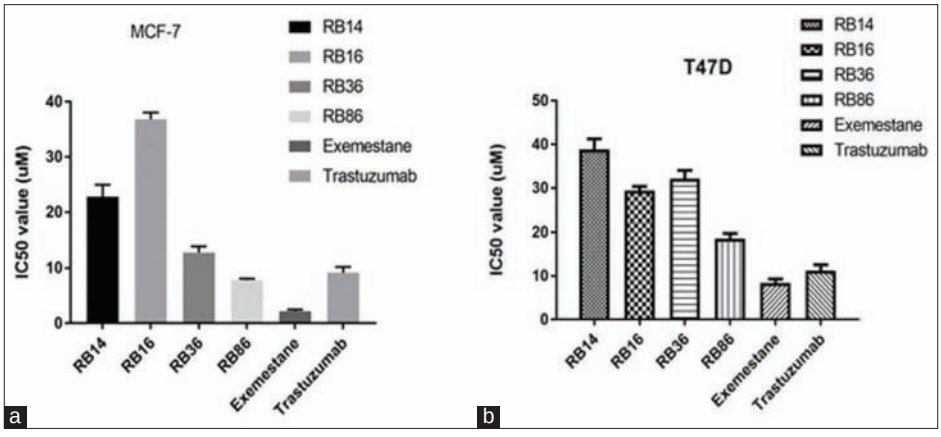

Figure 12: Cytotoxic activity of compounds against (a) MCF7 Cell lines (b) T47D Cell lines

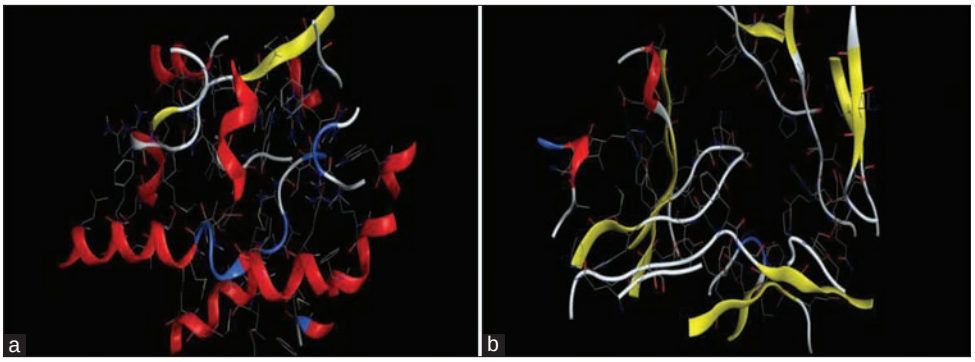

Figure 13: (a) Cavity of aromatase (PDB Id: 3S7S) (b) Cavity of HER2 (PDB Id: 3WSQ)

and root mean square value was determined by considering confirmation of internal ligand and re-docked confirmation. The docking scores of all the 90 ligands were determined against both the PDB Ids. Among the 90, top six with best scores for both the targets were selected which were further analyzed for determination of various types of interactions with the receptor amino acids in the best orientation and lowest energy state. Various types of interactions at particular distances were determined and compared with standard marketed drugs. The interaction poses and best orientation 3D poses were saved in JPEG format.

In silico drug likeliness prediction

Drug likeliness studies are significant to predict "drug like" behavior of the designed compounds and also helpful in predicting the bio-availability on the basis of physicochemical and structural properties. A compound can behave like a drug if it follows Lipinski's Rule of Five. It describes that for a compound to act as a potential therapeutic candidate, it must obey the five parameters: (a) Number of hydrogen bond donors should not be more than 5, (b) number of hydrogen bond acceptors should not be more than 10, (c) molecular mass should be <500 daltons, (d) number of rotatable bonds should not be less than 10, and (e) Log P (octanol-water partition coefficient) should not be greater than 5.[31] Drug likeliness properties were determined using swissADME software.

In silico ADME prediction

To exert maximum therapeutic action, a drug candidate must reach at its target site in sufficient concentration. Therefore, the preliminary idea about ADME properties of designed molecules is very much helpful in drug development. The ADME properties of the designed compounds were predicted using preADMET software. The compounds were evaluated for determination of absorption through HIA (human intestinal absorption), Caco-2 cell, MDCK (Maden Darby Canine Kidney), BBB, and plasma protein binding.[32]

In silico toxicity prediction

Toxicity prediction studies are very much helpful in predicting the toxicity of designed compounds on normal cells and tissues. These are also significant to determine the safe or toxic doses of a particular compound. These *in silico* predictions reduce the number of experimental animals, are cost effective and time saving. Two online softwares PreADME and Protox were used to predict the toxicity of designed compounds. PreADME predicts toxicity of compounds on carcino rats, carcino mice models, and Human Ether Related Gene factor (hERG). This hERG is associated with fatal cardiotoxicity.[33] Protox calculates the minimum lethal dose of the compounds on the basis of interactions of the compounds with various targets.[33]

Synthesis and characterization

Chemicals and reagents

All the solvents and reagents were procured from Sigma-Aldrich, Merck, and HiMedia and were used without further purification. Reactions were monitored by thin-layer chromatography (TLC) using commercially available precoated aluminum plates (Merck Kieselgel 60 F254 silica, 0.2 mm) with UV light (254 nm) and iodine as visualizing agents. Melting points were recorded with a COMPLAB melting point apparatus and were uncorrected. ^{1}H NMR and ^{13}C NMR spectra were recorded on a Bruker AM 300 (300 MHz) or a Bruker Avance III 500 (500 MHz; ^{13}C NMR at 75 and 125 MHz) spectrometer (Bruker Biosciences) using CDC_{l3} or DMSO-d_6 as the solvent at room temperature within the range. Chemical shifts (δ) are expressed as parts per million (ppm), using tetramethylsilane as the internal standard. Mass spectra were taken in ESI mode on an Agilent 1100 LC–MS.

Synthesis of coumarin-quinoxaline hybrids (12,13a dihydropyrano[3',2':5,6]indolo[2,3-b] quinoxalin-2(4a*H*)-ones)

A solution of 1.08 g of substituted o-phenylenediamine (**4**) and 1.95 g of isatin analogs (**3**) was heated overnight under reflux in 20 ml of glacial acetic acid. After cooling at room temperature, the reaction solvent was evaporated to half of its original volume. For most compounds the crude products get precipitated immediately. In the cases in which no precipitate appeared, the reaction mixture was poured into 25 ml of water. The resulting precipitate was filtered off, washed with ether, and purified by crystallization from methanol-acetic acid.

Characterization of synthesized compounds

Compound RB14 (4-methoxy-10-(trifluoromethyl)-12,13a-dihydropyrano[3',2':5,6]indolo[2,3-b] quinoxalin-2(4a*H*)-one

^{1}H NMR (300 MHz, $CDCl_3$) δ 3.5(s, 3H, OCH_3); 3.48 (s, 1H, CH); 10.08 (s, 1H, NH); 4.68(s, 1H, pyrone-CH);

7.62-7.85 (m, 3H, Ar-CH); 5.29-5.42 (m, 2H, Ph-CH); 6.16 (d, 1H, Ph-CH). **^{13}C NMR** (75 MHz, $CDCl_3$) δ 37.8, 56.2, 70.6, 89.5, 102.4, 124.4, 125.3, 125.7, 125.9, 126.8, 131.4, 132.8, 141.6, 144.8, 145.2, 148.9, 160.7, 162.4, 167.2.. **HRMS** (micro TOF-QII, MS, ESI): m/z $[M+H]^+$ Calculated for $C_{19}H_{12}F_3N_3O_3$ 387.08, Obsd. 388.29.

Compound RB 16 (4,9-dimethoxy-12,13a-dihydropyrano[3',2':5,6]indolo[2,3-b] quinoxalin-2(4a*H*)-one)

^{1}H NMR (300 MHz, $CDCl_3$) δ 3.55(s, 3H, OCH_3); 3.87(s, 3H, OCH_3); 3.48 (s, 1H, CH); 10.02 (s, 1H, NH); 4.67(s, 1H, pyrone-CH); 7.22-7.65 (m, 3H, Ar-CH); 5.27-5.32 (m, 2H, Ph-CH); 6.18 (d, 1H, Ph-CH). **^{13}C NMR** (75 MHz, $CDCl_3$) δ 37.8, 55.7, 55.9, 70.2, 88.5, 99.9, 102.4, 122.8, 125.6, 129.8, 131.1, 141.8, 141.5, 142.6, 149.2, 159.4, 160.6, 162.7, 166.1. **HRMS** (micro TOF-QII, MS, ESI): m/z $[M+H]^+$ Calculated for $C_{19}H_{15}N_3O_4$ 349.11, Obsd. 349.49.

Compound RB 36 (9-methoxy-4-phenyl-12,13a-dihydropyrano[3',2':5,6]indolo[2,3-b] quinoxalin-2(4a*H*)-one)

^{1}H NMR (300 MHz, $CDCl_3$) δ 3.87(s, 3H, OCH_3); 3.48 (s, 1H, CH); 10.02 (s, 1H, NH); 6.17(s, 1H, pyrone-CH); 7.12-7.59 (m, 3H, Ar-CH); 5.27-5.37 (m, 2H, Ph-CH); 6.80-7.28 (m, 5H, Ar-CH); 6.28 (d, 1H, Ph-CH). **^{13}C NMR** (75 MHz, $CDCl_3$) δ 39.2, 55.6, 73.8, 99.2, 102.6, 112.8, 122.6, 125.8, 126.6, 126.8, 127.8, 128.6, 128.6, 129.6, 130.2, 139.4, 141.6, 142.7, 142.9, 149.6, 154.6, 159.8, 160.4, 162.2. **HRMS** (micro TOF-QII, MS, ESI): m/z $[M+H]^+$ Calculated for $C_{24}H_{17}N_3O_3$ 395.11, Obsd. 395.79.

Compound RB 86 (4-hydroxy-5,9-dimethoxy-12,13a-dihydropyrano[3',2':5,6]indolo[2,3-b] quinoxalin-2(4a*H*)-one)

^{1}H NMR (300 MHz, $CDCl_3$) δ 3.87(s, 3H, OCH_3); δ 3.57(s, 3H, OCH_3); 3.48 (s, 1H, CH); 10.02 (s, 1H, NH); 6.77(s, 1H, pyrone-CH); 7.12-7.59 (m, 3H, Ar-CH); 5.27-5.37 (m, 2H, Ph-CH); 6.80-7.28 (m, 5H, Ar-CH); 6.28 (d, 1H, Ph-CH), 14.98 (s, 1H, OH) **^{13}C NMR** (75 MHz, $CDCl_3$) δ 42.2, 55.2, 56.9, 63.2, 92.5, 99.2, 102.8, 122.8, 129.6, 130.8, 142.8, 148.5, 154.6, 159.6, 160.2, 162.4, 197.7. **HRMS** (micro TOF-QII, MS, ESI): m/z $[M+H]^+$ Calculated for $C_{19}H_{15}N_3O_5$ 365.11, Obsd. 365.76.

Cytotoxic activity

The **MTT assay** is a colorimetric **assay** for measuring cell metabolic activity. It is based on the ability of nicotinamide adenine dinucleotide phosphate (NADPH)-dependent cellular oxidoreductase enzymes to reduce the tetrazolium dye **MTT** to its insoluble formazan, which has a purple color. The cytotoxicity induced by the new coumarin quinoxaline hybrids on breast cancer cell lines (MCF7 and T47D) was determined using MTT assay. Cell proliferation was estimated by MTT reduction by live cells when treated with synthesized compounds on MCF-7 and A549 cells. The marketed anticancer drugs exemestane and trastuzumab were used as standard drugs. Cells were seeded onto a 96-well plate at a concentration of 10^4 cells/well and allowed to adhere overnight. Five replicates were prepared for each treatment and cultured for 48 or 72 h. After 20 μL of MTT (5 mg/mL) was added to each well, the cells were cultured for another 4 h. The supernatant was discarded. After 150 μL of DMSO was added to each well, the samples were incubated at 37°C for 30 min and then swirled for 10 min. The absorbance at 570 nm was measured using a microplate reader. Experiments were repeated 3 times.

CONCLUSION

In this investigational study, we have hypothesized inhibitory potentials of coumarin-quinoxaline hybrids against aromatase and HER2 as both enzymes are associated with development and progression of breast cancer. A library of 90 hybrids was designed and docked against the two enzyme receptors and docking scores were screened out. Best seven hit compounds were further evaluated for particular types of interactions with the receptors. Hydrogen bonding, arene-cation, and arene-H interactions were found dominant. Further the compounds were analysed for drug likeliness and did not show any violation of Lipinski's Rule of Five. ADME prediction studies revealed that they have good absorption through human intestine and least through kidney cell lines. Furthermore, the compounds revealed least toxicity. The best four compounds **(RB14, RB16, RB36, and RB86)** were further synthesized and characterized by spectral techniques and were subjected to *in vitro* anti-breast cancer activity against MCF7 and T47D cell lines. Compound RB86 revealed maximum potency. The study was mainly aimed to investigate suitable therapeutic candidate by target based drug discovery approach. The evaluated best compounds may serve as new leads for further drug development.

REFERENCES

[1] Bhatia, R., Rawal, R.K. Coumarin hybrids: Promising scaffolds in the treatment of breast cancer, *Mini. Rev. Med. Chem.*, **2019**, *19*, 1443–1458.

[2] WHO. Available from: https://www.who.int/cancer/prevention/diagnosis-screening/breast-cancer/en. [Last accessed on 2020 Apr 15].

[3] Hua, H., Zhang, H., Kong, Q., Jiang, Y. Mechanisms for estrogen receptor expression in human cancer, *Exp. Hematol. Oncol*., **2018**, *7*, 1-11.

[4] Yaghjyan, L., Colditz, G.A. Estrogens in the breast tissue: A systematic review, *Cancer Causes Control*, **2011**, *22*, 529–540.

[5] Mukhopadhyay, K.D., Liu, Z., Bandyopadhyay, A., Kirma, N.B., Tekmal, R.R., Wang, S., Sun, L.Z. Aromatase expression increases the survival and malignancy of estrogen receptor positive breast cancer cells, *PLoS One*, **2015**, *10*, e0121136.

[6] Brueggemeier, R.W., Hackett, J.C., Diaz-Cruz, E.S. Aromatase inhibitors in the treatment of breast cancer, *Endocr. Rev.*, **2005**, *26*, 331–345.

[7] Bulun, S.E., Price, T.M., Aitken, J., Mahendroo, M.S., Simpson, E.R. A link between breast cancer and local estrogen biosynthesis suggested by quantification of breast adipose tissue aromatase cytochrome P450 transcripts using competitive polymerase chain reaction after reverse transcription, *J. Clin. Endocrinol. Metab*., **1993**, *77*, 1622–1628.

[8] McDonnell, D.P., Norris, J.D. Connections and regulation of the human estrogen receptor, *Science*, **2002**, *296*, 1642–1644.

[9] Smith, J. The third-generation aromatase inhibitors, *U S Pharm*., **2008**, *33*, 20–30.

[10] Freudenberg, J.A., Wang, Q., Katsumata, M., Drebin, J., Nagatomo, I., Greene, M.I. The role of HER2 in early breast cancer metastasis and the origins of resistance to HER2-targeted therapies, *Exp. Mol. Pathol*., **2009**, *87*, 1–11.

[11] Ménard, S., Tagliabue, E., Campiglio, M., Pupa, S.M. Role of HER2 gene overexpression in breast carcinoma, *J. Cell. Physiol.*, **2000**, *182*, 150–162.

[12] Clezardin, P. Therapeutic targets for bone metastases in breast cancer, *Breast Cancer Res*., **2011**, *13*, 207–215.

[13] Ravnan, M.C., Ravnan, S.L., Walberg, M.P. Metastatic breast cancer: A review of current and novel pharmacotherapy, *Formulary*, **2011**, *46*, 130–146.

[14] Cardoso, F., Senkus-Kone, E., Fallowfield, L., Costa, A., Castigilone, M. Locally recurrent or metastatic breast cancer: ESMO clinical practice guidelines for diagnosis, treatment and follow-up, *Ann. Oncol*., **2010**, *21*, 15–19.

[15] Pagani, O., Senkus, E., Wood, W., Colleoni, M., Cufer, T., Kyriakides, S., Costa, A., Winer, E.P., Cardoso, F. International guidelines for management of metastatic breast cancer: Can metastatic breast cancer be cured? *J. Natl. Cancer Inst*., **2010**, *102*, 456–463.

[16] Asadi, P., Khodarahmi, G., Jahanian-Najafabadi, A., Saghaie, L., Hassanzadeh, F. Biologically active heterocyclic hybrids based on quinazolinone, benzofuran and imidazolium moieties: Synthesis, characterization, cytotoxic and antibacterial evaluation, *Chem. Biodivers*., **2017**, *14*, 411.

[17] Yamaguchi, Y., Nishizono, N., Kobayashi, D., Yoshimura, T., Wada, K., Oda, K. Evaluation of synthesized coumarin derivatives on aromatase inhibitory activity, *Bioorg. Med. Chem. Lett*., **2017**, *27*, 2645–2649.

[18] Stefenachi, A., Favia, A.D., Nicolotti, O., Leonetti, F., Pisani, L., Catto, M., Zimmer, C., Hartmann, R.W., Carotti, A. Design, synthesis, and biological evaluation of imidazolyl derivatives of 4, 7 disubstituted coumarins as aromatase inhibitors selective over 17α-hydroxylase/c17-20 lyase, *J. Med. Chem*., **2011**, *54*, 1613–1625.

[19] Chen, S., Cho, M., Karlsberg, K., Zhou, D.Y., Yuan, C. Biochemical and biological characterization of a novel anti-aromatase coumarin derivative, *J. Biol. Chem*., **2004**, *279*, 48071–48078.

[20] Stefanachi, A., Leonetti, F., Pisani, L., Catto, M., Carotti, A. Coumarin: A natural, privileged and versatile scaffold for bioactive compounds, *Molecules*, **2018**, *23*, 250.

[21] El Newahie, A.M.S., Nissan, Y.M., Ismail, N.S.M., El Ella, D.A.A., Khojah, S.M., Abouzid, K.A.M. Design and synthesis of new quinoxaline derivatives as anticancer agents and apoptotic inducers, *Molecules*, **2019**, *24*, 1175.

[22] Bayoumi, A.H., Ghiaty, A.H., Abd-Ell-gill, S.M., Husseiny, E.M., Ebrahim, M.A. Exploration of quinoxaline derivatives as anti-microbial and anticancer agents, *J. Heterocycl. Chem.*, **2019**, *56*, 3215–3235.

[23] El Newahie, A.M.S., Ismail, N.S.M., El Ella, D.A.A., Abouzid, K.A. Quinoxaline-based scaffolds targeting tyrosine kinases and their potential anticancer activity, *Arch. Pharm.* (*Weinheim*), **2016**, *349*, 309–326.

[24] Unzue, A., Dong, J., Lafleur, K., Zhao, H., Frugier, E., Caflisch, A., Nevado, C. Pyrrolo [3, 2-b] quinoxaline derivatives as types I1/2 and II EPH tyrosine kinase inhibitors: Structure-based design, synthesis, and *in vivo* validation, *J. Med. Chem*., **2014**, *57*, 6834–6844.

[25] Kim, S.C., Boggu, P.R., Yu, H.N., Ki, S.Y., Jung, J.M., Kim, Y.S., Park, G.M., Ma, S.H., Kim, I.S., Jung, Y.H. Synthesis and biological evaluation of quinoxaline derivatives as specific c-Met kinase inhibitors, *Bioorg. Med. Chem. Lett.*, **2020**, *30*, 127189.

[26] Alswah, M., Bayoumi, A.H., Elgamal, K., Elmorsy, A., Ihmaid, S., Ahmed, H.E.A. Design, synthesis and cytotoxic evaluation of novel chalcone derivatives bearing triazolo [4, 3-a]-quinoxaline moieties as potent anticancer agents with dual EGFR kinase and tubulin polymerization inhibitory effects, *Molecules*, **2018**, **23**, 48.

[27] Sibiya, M.A., Raphoko, L., Mangokoana, D., Makola, R., Nxumalo, W., Matsebatlela, TM. Induction of cell death in human A549 cells using 3-(quinoxaline-3-yl) prop-2-ynyl methanosulphonate and 3-(quinoxaline-3-yl) prop-2-yn-1-ol, *Molecules*, **2019**, *24*, 407.

[28] Klein, L.L., Tufano, M.D. Synthesis of Substituted Isatins, Tetrahed Lett., 2013, 54(8), 1008-1011

[29] Sekhan, P., Storeng, R., Scudiero, D., Monks, A., McMahon, J., Vistica, D., Warren, J.T., Bokesch, H., Kenney, S., Boyd, M.R. New colorimetric cytotoxicity assay for anticancer-drug screening, *J. Natl. Cancer Inst*., **1990**, *82*, 1107–1112.

[30] Protein Data Bank. Available from: https://www.rcsb.org/pdb. [Last accessed on 2020 Apr 21].

[31] Lipinski, C.A., Lombardo, F., Dominy, B.W., Feeney, P.G. Experimental and computational approaches to estimate solubility and permeability in drug discovery and development settings, *Adv. Drug Deliv. Rev*., **2012**, *64*, 4–17**.**

[32] Lee, S.K., Chang, G.S., Lee, I.H., Chung, J.E., Sung, K.Y., No, K.T. The PreADME: PC-based program for batch prediction of ADME properties, *EuroQSAR*, **2004**, *9*, 5–10.

[33] Protox-II Prediction of Toxicity of Chemicals. Available from: http://www./tox.charite.de/protox_ii. [Last accessed on 2020 Apr 18].

Received: 03 May 2020; Accepted: 05 Aug 2020